# Atomic diffusion, step relaxation, and step fluctuations

B. Blagojević and P. M. Duxbury
*Department of Physics and Astronomy and Center for Fundamental Materials Research, Michigan State University, East Lansing, Michigan 48824-1116*
(Received 8 February 1999)

We show that the dynamics of the *pair correlation function* in a step train can pinpoint the dominant relaxation mechanism occurring at a crystal surface. Evaporation-condensation and step-edge diffusion do not produce dynamical correlations between neighboring steps, while terrace diffusion may lead to correlations which fall off like a power law with distance and which are peaked at a characteristic time. We derive these results within a ''real space'' Langevin formalism which is based on diffusion kernels which are different for each mass transport process. We validate this formalism by reproducing the step fluctuation autocorrelation function. We then derive results on the pair correlation between different steps. Results for solvable limiting cases are summarized in Tables I and II of the paper. As an intermediate step in the analysis we also find expressions for the relaxation time $\tau_{pq}$ of a mode of wave number $q$ along the steps and wave number $p$ perpendicular to the steps, which we also discuss and compare with prior work. [S1063-651X(99)06907-X]

PACS number(s): 05.40.−a, 68.35.Bs, 68.35.Ja

## I. INTRODUCTION

Steps are the most fundamental extended defects on crystal surfaces. Their dynamics mediate the annealing of crystal surfaces, the growth of single crystals, and many other surface processes [1]. Step dynamics are in turn mediated by atom motion, usually either evaporation and condensation from a vapor, diffusion across terraces or facets, or by diffusion along step edges. The high resolution provided by scanning tunneling microscopy (STM) and reflection electron microscopy (REM) is providing atomic scale images of stochastic step fluctuations [2–7]. Understanding of these data requires a quantitative analysis of step fluctuations in terms of the atomic processes producing them [8–13]. Such theory, in combination with high quality step fluctuation data, provides a unique method for determining the dominant modes of mass transport across surfaces, and for estimating the energy barriers which impede the various atomic processes contributing to them. A complementary probe of atomic diffusion processes is the study of the decay of specially prepared surface gratings, which in the small slope limit are described by a closely related theory [14,15].

Current measurements and theory concentrate on the fluctuations of a step belonging to a step train, $G(t)$. A simple physical interpretation of $G(t)$ is the mean square distance a point on a step diffuses as a function of time. At very short times the motion is often diffusive [$G(t)\sim t$], but very quickly the motion becomes subdiffuse due to the fact that a point on a step edge is connected to other points on the step edge and hence its motion is impeded. The exponent of this subdiffuse motion is related to the dominant mode of atomic transport, and the prefactors are related to the energy barriers. The analysis of $G(t)$, however, is often ambiguous as its behavior is quite similar for different atomic diffusion mechanisms [9,11,16,13].

Here we generalize the analysis of step fluctuation correlations by studying the $x$ dependence of correlations on the same step [i.e., $G(x,t)$], and more importantly by analyzing the *pair correlation function* between two steps $C_k(x,t)$. $C_k(x,t)$ is an averaged product of the fluctuations of two step positions separated by distance $x$ parallel to the step edge and located $k$ steps apart. In order to calculate $C_k(x,t)$ and $G(x,t)$, we first calculate the relaxation time $\tau_{pq}$ for steps which are modulated along the steps (with wave number $q$), and perpendicular to the steps (with wave number $p$). By summing over all modes, with the correct matrix elements, we then derive $C_k(x,t)$ and $G(x,t)$. $C_{k\neq 0}(x,t)$ is identically zero for the cases of evaporation-condensation and step-edge diffusion. In contrast, $C_{k\neq 0}(x,t)$ is finite and quite large in the case of terrace diffusion. This means that measurement of a finite value for $C_{k\neq 0}(x,t)$ implies that terrace diffusion is important. Since $G(t)$ quantifies the cumulative effect of *all mass transport mechanisms*, by combining the results of $G(t)$ and $C_{k\neq 0}(x,t)$ it is then possible to determine the relative importance of terrace diffusion as compared to the other types of surface mass transport.

Our calculations use a real space Langevin formalism which provides a nice physical picture of the diffusion processes contributing to mass transport on stepped surfaces, and also relates the sticking coefficients and kinetic parameters more directly to step edge and terrace energy barriers. A preliminary discussion of this formalism and results for $G(0,t)$ have appeared as a conference proceedings [11].

The paper is arranged as follows. Section II contains the real space formulation of step dynamics, with the key equations being Eq. (17) for the relaxation time $\tau_{pq}$ and Eq. (24) for the correlation function $C_k(x,t)$. Section III contains an analysis of $C_k(x,t)$ and $G(x,t)$ in a variety of time regimes. This section can be skipped by those uninterested in the detailed analysis. Section IV treats cases of physical interest, in particular evaporation-condensation, step-edge diffusion and terrace diffusion. Analytic results for $G(0,t)$ and $C_k(0,t)$ for solvable limiting cases are summarized in Tables I and II, respectively. Examples illustrating some of the more interesting crossovers between these limiting cases are illustrated in Figs. 3 and 4. Section V contains a brief conclusion.

 

TABLE I. Limiting behaviors for $G(0,t)$.

| Mass transport mechanism | Time regime | $G(0,t)$ |
|---|---|---|
| Evaporation-condensation (EC) | $t\to 0$ | $\sim t$ |
| | $0\ll t\ll \tau_s^{\mathrm{ST}}$ | $\Omega\left(\frac{a_\perp}{\pi\tilde{s}}\right)^{1/2}\left(\frac{t}{\tau_{\mathrm{EC}}}\right)^{1/2}$ |
| | $t\gg \tau_s^{\mathrm{ST}}$ | $\frac{L\Omega}{12\tilde{s}}\left(1-\frac{6}{\pi^2}e^{-t/\tau_s^{\mathrm{EC}}}\right)$ |
| Step-edge diffusion (SE) | $t\to 0$ | $\sim t$ |
| | $0\ll t\ll \tau_s^{\mathrm{SE}}$ | $\frac{\Gamma(\frac{3}{4})}{\pi}\left(\frac{\Omega^5 a_\parallel}{\tilde{s}^3}\right)^{1/4}\left(\frac{t}{\tau_{\mathrm{SE}}}\right)^{1/4}$ |
| | $t\gg \tau_s^{\mathrm{SE}}$ | $\frac{L\Omega}{12\tilde{s}}\left(1-\frac{6}{\pi^2}e^{-t/\tau_s^{\mathrm{SE}}}\right)$ |
| Terrace diffusion 1 ($T1$) | $t\to 0$ | $\sim t$ |
| $d\to\infty$ | $0\ll t\ll t_1^{T1}$ | $\Omega a_\perp\left(\frac{\alpha_U+\alpha_L}{\pi\tilde{s}}\right)^{1/2}\left(\frac{t}{\tau_{\mathrm{TD}}}\right)^{1/2}$ |
| (isolated step) | $t_1^{T1}\ll t\ll t_2^{T1}$ | $\frac{\Omega\Gamma(\frac{2}{3})}{\pi}\left(\frac{a_\perp^2}{\tilde{s}^2}\right)^{1/3}\left(\frac{t}{\tau_{\mathrm{TD}}}\right)^{1/3}$ |
| | $t_2^{T1}\ll t\ll \tau_s^{T1}$ | $\frac{\Omega\Gamma(\frac{2}{3})}{\pi}\left(\frac{2a_\perp^2}{\tilde{s}^2}\right)^{1/3}\left(\frac{t}{\tau_{\mathrm{TD}}}\right)^{1/3}$ |
| | $t\gg \tau_s^{T1}$ | $\frac{L}{12\tilde{s}}\left(1-\frac{6}{\pi^2}e^{-t/\tau_s^{T1}}\right)$ |
| Terrace diffusion 2 ($T2$) | $t\ll t_1^{T2}$ | as for isolated step ($T1$) |
| $d$ finite, $\alpha_U=0$ or $\alpha_L=0$ | $t_1^{T2}\ll t\ll \tau_s^{T2}$ | $\frac{\Omega\Gamma(\frac{3}{4})}{\pi}\left(\frac{da_\perp^2}{\tilde{s}^3}\right)^{1/4}\left(\frac{t}{\tau_{\mathrm{TD}}}\right)^{1/4}$ |
| (e.g., Schwoebel barrier $=\infty$) | $t\gg \tau_s^{T2}$ | $\frac{L}{12\tilde{s}}\left(1-\frac{6}{\pi^2}e^{-t/\tau_s^{T2}}\right)$ |
| Terrace diffusion 3 ($T3$) | $t\ll t_1^{T3}$ | as for isolated step ($T1$) |
| $d$ finite, $\alpha_{U,L}\neq 0$ | $t_1^{T3}\ll t\ll \tau_s^{T3}$ | $4\Omega a_\perp\left(\frac{1}{\pi^3\tilde{s}(d+d_0)}\right)^{1/2}\left(\frac{t}{\tau_{\mathrm{TD}}}\right)^{1/2}$ |
| | $t\gg \tau_s^{T3}$ | $\frac{L\Omega}{12\tilde{s}}\left\{1-\frac{3L}{2\pi^3}\left(\frac{d+d_0}{\pi a_\perp^2\tilde{s}}\right)^{1/2}\left(\frac{t}{\tau_{\mathrm{TD}}}\right)^{-1/2}e^{-(2\pi/L)^4\tilde{s}a_\perp^2 dt/\tau_{\mathrm{TD}}}\right\}$ |

## II. MODEL

Consider a train of $N$ steps, all with length $L$ (see Fig. 1). We number the steps with $k=1,2,\ldots,N$, and assume periodic boundary conditions both along the step train and along each step (this simplifies the analysis and is typical of steps away from the edges of a finite step train). Let $h_k(x,t)$ describe the random motion of the $k$th step in the train about its *center of mass*, which is assumed to be *fixed* — there are no ''direct'' interaction terms to produce center of mass dynamics. The average distance between centers of mass of adjacent steps is the same everywhere on the surface and equals $d$.

Let us define the equilibrium ($t\ll t_1\to\infty$) correlation functions

$$G(x,t)=\tfrac{1}{2}\langle[h_{k_1}(x_1+x,t_1+t)-h_{k_1}(x_1,t_1)]^2\rangle \qquad (1)$$

and

$$C_k(x,t)=\langle h_{k_1+k}(x_1+x,t_1+t)h_{k_1}(x_1,t_1)\rangle. \qquad (2)$$

$G(x,t)$ measures fluctuations, while $C_k(x,t)$ measures correlations. Because of the periodic boundaries, $G(x,t)$ and $C_k(x,t)$ do not depend on $x_1$ and $k_1$. By squaring the bracket

TABLE II. Limiting behaviors for $C_{k\neq 0}(0,t)$.

| Mass transport mechanism | Time regime | $C_{k\neq 0}(t)$ |
|---|---|---|
| Terrace diffusion 3 ($T3$) | $t\rightarrow 0$ | $\frac{\Omega d}{2\pi\tilde{s}k!(2k-1)}\left(\frac{4\tilde{s}a_\perp^2}{(d+d_0)d^2}\right)^k\left(\frac{t}{\tau_{\rm TD}}\right)^k$ |
| $d$ finite, $\alpha_{U,L}\neq 0$ | $0\ll t\ll\tau_s^{T3}$ | $\frac{4\Omega}{4k^2-1}\left(\frac{a_\perp^2}{(d+d_0)\pi^3\tilde{s}}\right)^{1/2}\left(\frac{t}{\tau_{\rm TD}}\right)^{1/2}$ |
| | $t\gg\tau_s^{T3}$ | $\frac{\Omega L^2}{8\tilde{s}\pi^3}\left(\frac{d+d_0}{\pi a_\perp^2\tilde{s}}\right)^{1/2}\left(\frac{t}{\tau_{\rm TD}}\right)^{-1/2}e^{-(2\pi/L)^4\tilde{s}a_\perp^2 d(t/\tau_{\rm TD})}$ |

in Eq. (1) and taking an average of each term individually, we find that these two functions are related as

$$G(x,t)=C_0(0,0)-C_0(x,t), \tag{3}$$

where $C_0(0,0)$ is the squared equilibrium width of a step.

The local chemical potential, $\mu_k(x,t)$, which we associate with the $k$th step, is

$$\mu_k(x,t)=-\Omega\tilde{\Sigma}\nabla^2 h_k(x,t). \tag{4}$$

It is derived using

$$F_k\approx\frac{\tilde{\Sigma}}{2}\int_{-L/2}^{L/2}(\nabla h_k)^2 dx \tag{5}$$

as the energy cost of Gaussian fluctuations of the step edge about its mean position [17]. $\Omega=a_\perp a_\parallel$ is the area of a surface element, with $a_\perp$ and $a_\parallel$ being the lattice spacings perpendicular and parallel to the step edge, respectively. We describe the time dependent fluctuations of the steps using a coupled set of Langevin equations,

$$\frac{\partial h_k(x,t)}{\partial t}=\frac{\Gamma_h}{k_BT}\left\{\frac{1}{2}J_{k-1,k}(x,t)+J_{k,k}(x,t)+\frac{1}{2}J_{k+1,k}(x,t)\right\}+\eta_k(x,t). \tag{6}$$

$J_{k,k}$ describes the healing of the step fluctuation due to mass transport along a step, while $J_{k-1,k}$ and $J_{k+1,k}$ describe the healing of such fluctuations due to mass transport between step $k$ and steps $k-1$ and $k+1$, respectively. The healing of fluctuations is driven by differences in the step chemical potential, and the rate of that healing is controlled by the rate at which mass may be transferred in order to heal unfavorable chemical potential differences. The rate

$$\Gamma_h=\frac{a_\perp}{\tau_h}, \tag{7}$$

where $\tau_h$ is the time between detachment events, depends on the energy barriers which exist at the step edges. We shall discuss this further in the context of specific types of mass transport.

Considering first healing due to mass transport along a step edge, the integral $J_{k,k}$ is given by

$$J_{k,k}(x,t)=\int_0^{L/2}P_0(l)\{\mu_k(x+l,t)-2\mu_k(x,t)+\mu_k(x-l,t)\}dl, \tag{8}$$

where the chemical potential difference between sites separated by distance $l$ is contained in the curly brackets, and the ''mobility'' is described by $P_0(l)$. This mobility is the probability that an atom is exchanged between two sites separated by distance $l$ along the $x$ axis and located on the same step edge. In the case of evaporation-recondensation, $P(l)$ is a constant independent of $l$, in the terrace diffusion case, $P_0(l)$ is calculated from the diffusion equation with the boundary conditions at the step edges being related to lattice sticking coefficients. The form of $P_0(l)$ depends on the mass transport mechanism, as we elucidate later in Sec. IV. However we can do the analysis to a large degree without knowing the explicit form for the mobilities [the curious reader may look at Eqs. (46) or (49) for some examples of $P_0(l)$]. The integral describing the way in which fluctuations heal due to mass transport between steps is very similar to Eq. (8):

$$J_{k\pm 1,k}(x,t)=\int_0^{L/2}P_1(l)\{\mu_{k\pm 1}(x+l,t)-2\mu_k(x,t)+\mu_{k\pm 1}(x-l,t)\}dl. \tag{9}$$

$P_1(l)$ is the probability that an atom is exchanged between two sites separated by a distance $l$ along the $x$ axis but located on the adjacent step edges, and is calculated in a similar manner to $P_0(l)$. The probability functions are even and normalized,

$$2\int_0^{L/2} dl(P_0(l)+P_1(l))=1. \tag{10}$$

Step perturbations or fluctuations are randomly generated by the noise term $\eta_k(x,t)$ and then healed by the processes described in the integrals $J_{k,k}$ and $J_{k\pm1,k}$. The noise must be constructed so that the time independent equilibrium properties of the steps are reproduced. Since we assume that there are no interactions between steps, the equilibrium correlations of the step train are simply those of noninteracting steps. We shall return to this later.

A Fourier transform

$$h_k(x,t)=\sum_q h_{kq}(t)e^{iqx}, \tag{11}$$

and similarly for $\eta_k(x,t)$, with $q=2\pi n/L$ and $n=\pm1,\pm2,\ldots,\pm L/a_\parallel$ in Eq. (6), yields the $N$-dimensional set of linear first-order differential equations:

$$\frac{\partial \vec{h}_q(t)}{\partial t}=-\tilde{M}(q)\vec{h}_q(t)+\vec{\eta}_q(t), \tag{12}$$

with $\tilde{M}$ given by

$$\tilde{M}(q)=\begin{pmatrix} g_0(q) & -\frac{1}{2}g_1(q) & 0 & \cdots & -\frac{1}{2}g_1(q) \\ -\frac{1}{2}g_1(q) & g_0(q) & -\frac{1}{2}g_1(q) & \cdots & 0 \\ \vdots & \ddots & \ddots & \ddots & \vdots \\ 0 & \cdots & -\frac{1}{2}g_1(q) & g_0(q) & -\frac{1}{2}g_1(q) \\ -\frac{1}{2}g_1(q) & \cdots & 0 & -\frac{1}{2}g_1(q) & g_0(q) \end{pmatrix}, \tag{13}$$

where

$$g_0(q)=\frac{\tilde{s}q^2a_\perp}{\tau_h}\left\{1-2\int_0^{L/2}P_0(l)\cos ql\,dl\right\},$$

$$g_1(q)=\frac{2\tilde{s}q^2a_\perp}{\tau_h}\int_0^{L/2}P_1(l)\cos ql\,dl, \tag{14}$$

with the reduced stiffness $\tilde{s}=\tilde{\Sigma}\Omega/k_BT$ having units of length.

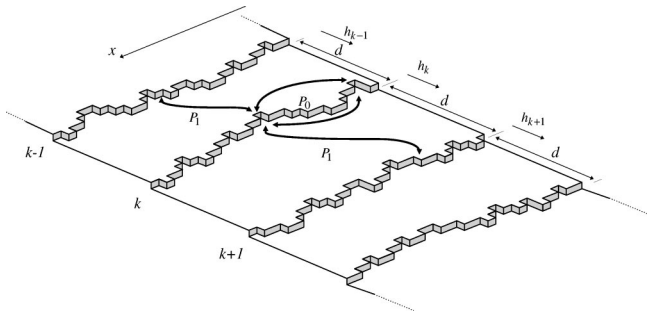


FIG. 1. Diffusion kernels on a vicinal surface.

In order to decouple the system of equations (12), we need to diagonalize the matrix $\tilde{M}$. Since this matrix is circulant [18], it is also diagonalized by a Fourier transform,

$$\vec{v}_q(t)=\tilde{U}^+\vec{h}_q(t) \quad \text{with} \quad U_{km}=\frac{1}{\sqrt{N}}e^{i(k-1)p} \tag{15}$$

where $p=2\pi m/N$, $m=0,1,2,\ldots,N-1$. When this is completed, we arrive at a set of decoupled linear Langevin equations

$$\frac{\partial v_{pq}(t)}{\partial t}=-\frac{v_{pq}(t)}{\tau_{pq}}+\eta_{pq}(t), \tag{16}$$

where each mode $(p,q)$ has a relaxation time $\tau_{pq}$ given by

$$\tau_{pq}^{-1}=g_0(q)-g_1(q)\cos p, \tag{17}$$

and is associated with the noise $\eta_{pq}(t)$. The statistics of the noise is unaltered, and therefore we can keep the same symbol $\vec{\eta}$. In the absence of noise, Eq. (16) describes the relaxation of a periodic mode (e.g., sinusoidal with wave number $q$ along the steps and $p$ perpendicular to the steps) with relaxation time $\tau_{pq}$. This mode relaxes as

$$v_{pq}(t)=v_{pq}(0)e^{-t/\tau_{pq}}, \tag{18}$$

where $v_{pq}(0)$ is the initial (small) amplitude of the mode.

We are now ready to calculate the key correlation function $C_k(x,t)$. First we solve the linear Langevin equation (16),

$$v_{pq}(t)=e^{-t/\tau_{pq}}\int_0^t e^{t'/\tau_{pq}}\eta_{pq}(t')dt'. \tag{19}$$

Then

$$\langle v_{p_1q_1}(t_1)v_{p_2q_2}(t_2)\rangle = e^{-t_1/\tau_{p_1q_1}-t_2/\tau_{p_2q_2}} \times\int_0^{t_1}\int_0^{t_2} e^{t_1'/\tau_{p_1q_1}+t_2'/\tau_{p_2q_2}} \times\langle \eta_{p_1q_1}(t_1')\eta_{p_2q_2}(t_2')\rangle dt_1'dt_2'. \tag{20}$$

To proceed further, we need to decide on a form for the noise. We choose Gaussian white noise, in which case

$$\langle \eta_{p_1q_1}(t_1)\eta^*_{p_2q_2}(t_2)\rangle = f(p_1,p_2,q_1,q_2)\delta_{p_1,p_2}\delta_{q_1,q_2}\delta(t_1-t_2). \tag{21}$$

Evaluating Eq. (20) using this form of the noise leads to

$$\langle v_{pq}(t_1)v^*_{pq}(t_2)\rangle = \frac{f(p,q)\tau_{pq}}{2}(e^{(t_1-t_2)/\tau_{pq}}-e^{-(t_1+t_2)/\tau_{pq}}). \tag{22}$$

Taking the limit $t_1\to\infty$ and setting $t_2-t_1=t$, we obtain

$$\langle v_{pq}(t_1)v^*_{pq}(t_1+t)\rangle = \frac{f(p,q)\tau_{pq}}{2}e^{-t/\tau_{pq}}. \tag{23}$$

We reconstruct the key correlation function $C_k(x,t)$ by inverting the Fourier transforms (11) and (15) as

$$C_k(x,t)=\frac{\Omega}{NL\tilde{s}}\sum_q \frac{\cos qx\, e^{-g_0(q)t}}{q^2}\sum_p \cos pk\, e^{g_1(q)t\cos p}, \tag{24}$$

where $p=2\pi m/N$, $m=0,1,2,\ldots,N-1$, and $q=2\pi n/L, n=\pm1,\pm2,\ldots,\pm L/a_\parallel$. In finding Eq. (24), we have also set $f(p,q)=2\Omega/(\tilde{s}Lq^2\tau_{pq})$. This choice is necessary so that $C_0(0,0)$ reproduces the squared equilibrium width $L\Omega/12\tilde{s}$ [19].

Section III presents an analysis of Eq. (24) in a variety of solvable limits. This section is used in Sec. IV which discusses physical cases, but may be skipped by those uninterested in a detailed analysis.

### III. ANALYSIS OF VARIOUS TIME REGIMES

Taking the continuum limit of the $p$ sum gives (p. 376-9.6.19 of Ref. [20]),

$$C_k(x,t)=\frac{2\Omega}{L\tilde{s}}\sum_{q>0}\frac{\cos qx\, e^{-g_0(q)t}}{q^2}I_k(g_1(q)t), \tag{25}$$

where $I_k(z)$ is the modified Bessel function of order $k$ and argument $z$. To make the analysis in this section simpler, we will consider a summation over positive $q$ only.

At $t=0$, Eq. (25) reduces [because $I_{k\neq0}(0)=0$ and $I_0(0)=1$; p. 375-9.6.7 of Ref. [20]] to [p. 39-1.443(3) of Ref. [21]]

$$C_0(x,0)=\frac{L\Omega}{2\tilde{s}}\left(\frac{1}{6}-\frac{x}{L}+\left(\frac{x}{L}\right)^2\right), \tag{26}$$

which is the equilibrium correlation function along a step, while the equilibrium correlations between steps are zero $[C_{k\neq0}(x,0)=0]$. The equilibrium correlations between steps $C_{k\neq0}(x,0)$ are zero due to the fact that there are no direct energy terms between steps in our model. Nevertheless, as demonstrated below, there are strong *time dependent correlations* $C_{k\neq0}(x,t>0)$ between steps when there is correlated mass transport across the terraces (e.g., terrace diffusion). These correlations are absent in the case of evaporation-condensation and step-edge diffusion. The analysis of the correlations between different steps thus provides a method to distinguish between evaporation-condensation and terrace diffusion, which have very similar trends in the correlation function on the same step.

Due to the difference between the equilibrium behavior of the correlation functions between the same steps and different steps, we treat these two cases differently. For correlations between different steps we use $C_{k\neq0}(x,t)$, which increases from zero at short time. For the step self-correlation, we use $G(x,t)$ which also increases from zero at short time, rather then $C_0(x,t)$ which starts at its equilibrium value. This is more convenient when testing for the power law behaviors so typical of step dynamics.

To proceed to an analytic analysis of the time dependence of $C_{k\neq0}(x,t)$ and $G(x,t)$, we need more detailed expressions for $g_0(q)$ and $g_1(q)$. We show in Sec. IV that the important asymptotic behaviors of these functions can be expressed in relatively simple forms. There are two cases; one is for terrace diffusion (case A) and the other applies to evaporation-condensation, step-edge diffusion, or terrace diffusion with an infinite Schwoebel barrier (case B).

In case A (terrace diffusion),

$$g_0(q)\approx A_1|q|^{\gamma_1}+B|q|^{\beta},\quad g_1(q)\approx A_1|q|^{\gamma_1}\quad \text{for}\quad |q|<q_0,$$
$$g_0(q)\approx A_2|q|^{\gamma_2},\quad g_1(q)=0\quad \text{for}\quad |q|>q_0. \tag{27}$$

For $|q|<q_0$, $B|q|^{\beta}\ll A_1|q|^{\gamma_1}$ is always satisfied, and we will neglect term $B|q|^{\beta}$ in the following calculation except in the expression $g_0(q)-g_1(q)$.

In case B (evaporation-condensation, step-edge diffusion, or terrace diffusion with an infinite Schwoebel barrier),

$$g_0(q)\approx A_1|q|^{\gamma_1},\quad g_1(q)=0\quad \text{for}\quad |q|<q_0,$$
$$g_0(q)\approx A_2|q|^{\gamma_2},\quad g_1(q)=0\quad \text{for}\quad |q|>q_0. \tag{28}$$

The details of the system of interest (terrace width, energies, diffusion constants, etc.) are primarily contained in the prefactors $A_{1,2}$, the crossover wave number $q_0$, and the lower limit of $q=2\pi/L$. The exponents $\gamma_{1,2}$ take on quite universal values depending on the mass transport mecha-

nism. Nevertheless we now do a complete asymptotic analysis without knowing these details, and then use those results in Sec. IV. In Sec. IV we also compare these asymptotic results with direct numerical evaluations of Eq. (24) for physically interesting cases.

There are three important asymptotic time regimes in the step dynamics: (i) early times $t\to 0$, (ii) intermediate times $0\ll t\ll \tau_s$, and (iii) very long times $t\gg\tau_s$. Here, the characteristic time

$$\tau_s=(L/2\pi)^{\gamma_1}/A_1 \tag{29}$$

is the decay time of slowest mode in the system. We present the asymptotic forms for $C_{k\neq 0}(x,t)$ and $G(x,t)$ in these three regimes, though frequently (ii) is the most experimentally accessible one.

### A. Correlations between different steps — $C_{k\neq 0}(x,t)$ (only case A)

Starting from zero at $t=0$, the correlation between steps $C_{k\neq 0}(x,t)$ grows due to correlated mass transport between steps. Neither step-edge diffusion, evaporation-condensation, nor terrace diffusion with an infinite Schwoebel barrier (case B) produce this correlation, so $C_{k\neq 0}(x,t)=0$ in these cases. Considering case A [Eq. (27)], sum (25) ceases to contribute for $q>q_0$, due to the fact that the Bessel function $I_{k\neq 0}(0)=0$. We then have [combining Eqs. (25) and (27)]

$$C_{k\neq 0}(x,t)=\frac{2\Omega}{L\tilde{s}}\sum_{q<q_0}\frac{\cos qx\, e^{-A_1 q^{\gamma_1}t}}{q^2}I_k(A_1q^{\gamma_1}t). \tag{30}$$

(i) *Short times* $t\to 0$. At short times, we expand the Bessel function for small argument (p. 375-9.6.7 of Ref. [20]),

$$I_k(z)=\left(\frac{z}{2}\right)^k\frac{1}{k!},\quad z\to 0, \tag{31}$$

and set the exponential to 1, which yields

$$C_{k\neq 0}(x,t)=\frac{2\Omega}{L\tilde{s}}\sum_{q<q_0}\frac{\cos qx}{q^2}\frac{(A_1q^{\gamma_1}t)^k}{2^k k!}. \tag{32}$$

This is valid provided $t\ll 1/(A_1q_0^{\gamma_1})$. Turning the sum into an integral and evaluating shows that at small $x$ we have

$$C_{k\neq 0}(x,t)=\frac{\Omega}{\tilde{s}\pi}\frac{q_0^{k\gamma_1-1}}{k!(k\gamma_1-1)}\left(\frac{A_1t}{2}\right)^k,\quad q_0x\to 0. \tag{33}$$

(ii) *Intermediate times* $0\ll t\ll\tau_s$. In this regime, sum (25) is dominated by small $q$, so we can take the upper limit to $\infty$. However, all values of $q$ contribute, so we can take the continuum limit and, rewriting in terms of more convenient variables, we then find

$$C_{k\neq 0}(x,t)=\frac{\Omega}{\pi\tilde{s}}\frac{(A_1t)^{1/\gamma_1}}{\gamma_1}\times\int_0^\infty\frac{e^{-y}\cos\left(x\left(\frac{y}{A_1t}\right)^{1/\gamma_1}\right)I_k(y)}{y^{1+1/\gamma_1}}dy. \tag{34}$$

For small $x$, the cosine tends to unity, and the integral may be written in terms of $\gamma$ functions (p. 486-11.4.13 of Ref. [20]),

$$C_{k\neq 0}(x,t)=\frac{\Omega}{\tilde{s}\pi^{3/2}}\frac{2^{1/\gamma_1}\Gamma\left(k-\frac{1}{\gamma_1}\right)\Gamma\left(\frac{1}{2}+\frac{1}{\gamma_1}\right)}{\gamma_1\Gamma\left(k+\frac{1}{\gamma_1}+1\right)}(A_1t)^{1/\gamma_1},\quad x\to 0. \tag{35}$$

(iii) *Long time limit* $t\gg\tau_s$. We may then use the large argument expansion for the Bessel function (p. 377-9.7.1 of Ref. [20])

$$I_k(z)\approx\frac{e^z}{(2\pi z)^{1/2}}. \tag{36}$$

Now the small correction $B|q|^\beta$ is the only term that survives in Eq. (25). The first term in the sum is dominant; thus, for small $x$,

$$C_k(x,t)\approx\frac{2\Omega}{L\tilde{s}}\left(\frac{L}{2\pi}\right)^{2+\gamma_1/2}\frac{e^{-B(2\pi/L)^\beta t}}{(2\pi A_1t)^{1/2}},\quad \frac{x}{L}\to 0. \tag{37}$$

A surprising feature of this expression is that it is independent of $k$, indicating that asymptotically all of the steps are correlated in the same way. It is also valid for $k=0$, i.e., correlations on the same and different steps decay at long times in the same manner.

### B. Correlations on the same step — $G(x,t)$ (both cases A and B)

We consider [combining Eqs. (3) and (25)]

$$G(x,t)=\frac{2\Omega}{L\tilde{s}}\sum_q\frac{1-\cos qx\, e^{-g_0(q)t}I_0(g_1(q)t)}{q^2}. \tag{38}$$

First, we analyze this equation for small $x$ (when the cosine tends to unity) for three time regimes.

(i) *Short times* $t\to 0$. At short times, using $I_0(0)=1$ and $g_0(q)=A_1q^{\gamma_1}$ for $q<q_0$, $g_0(q)=A_2q^{\gamma_2}$ for $q>q_0$, and expanding the exponential in Eq. (38) to the second order, we find

$$G(x\to 0,t)=\frac{\Omega}{\pi\tilde{s}}\left(A_1\frac{q_0^{\gamma_1-1}}{\gamma_1-1}+A_2\frac{(2\pi/a_\parallel)^{\gamma_2-1}-q_0^{\gamma_2-1}}{\gamma_2-1}\right)t \tag{39}$$

for both the cases A and B.

(ii) *Intermediate times* $0 \ll t \ll \tau_s$. This regime actually breaks up into two regimes. The first, $0 \ll t \ll t_x$, is dominated by the modes in the regime $q \gg q_0$, while the second, $t_x \ll t \ll \tau_s$, is dominated by modes in the regime $q \ll q_0$. These regimes are quite distinct due to the fact that $\tau_{pq}$ only appears in the exponential. It is then quite a good approximation to treat the first time regime using $A_2 q^{\gamma_2}$, and the later time regime using $A_1 q^{\gamma_1}$. We do an analysis similar to that leading to Eq. (34) to find

$$G(x \to 0,t) = \frac{\Omega}{\tilde{s}\pi} \Gamma\left(1 - \frac{1}{\gamma_2}\right) (A_2 t)^{1/\gamma_2}, \quad t \ll t_x, \tag{40}$$

for both cases A and B, and

$$G(x \to 0,t) = C \frac{\Omega}{\tilde{s}\pi} \Gamma\left(1 - \frac{1}{\gamma_1}\right) (A_1 t)^{1/\gamma_1}, \quad t \gg t_x, \tag{41}$$

where $C = (2^{1/\gamma_1} \gamma_1 \Gamma(1/2 + 1/\gamma_1))/(\sqrt{\pi}\Gamma(1/\gamma_1))$ (integration by parts using p. 486-11.4.13 of Ref. [20]) for case A, and $C = 1$ [p. 333-3.434(1) of Ref. [21]] for case B. The crossover time $t_x$ is found by equating Eqs. (40) and (41), and solving for the time. In the physical cases, there may be several different crossovers in this intermediate time regime, but the same general principles can be applied. Naturally this complexity makes experimental data difficult to analyze in general.

(iii) *Long times* $t > \tau_s$. We first find $C_0(x \to 0,t)$ for long times. In case A, it is given by Eq. (37). In case B, the argument of the Bessel function in Eq. (25) is zero. We then have $I_0(0) = 1$, and, since the first term in the sum is dominant,

$$C_0(x \to 0,t) \approx \frac{2\Omega}{L\tilde{s}} \left(\frac{L}{2\pi}\right)^2 e^{-t/\tau_s}, \tag{42}$$

whose time scale is set by the slowest mode in the system, $\tau_s$. Then, using Eq. (3),

$$G(x \to 0,t) = \frac{L\Omega}{12\tilde{s}} - C_0(x \to 0,t). \tag{43}$$

For larger $x$ we find, combining Eqs. (3) and (26),

$$G(x \neq 0,t) = \frac{\Omega x}{2\tilde{s}} \left(1 - \frac{x}{L}\right) \tag{44}$$

for short times. On the other hand, we find $G(x \neq 0,t) = G(0,t)$ for longer times. Therefore, $G(x \neq 0,t)$ is initially constant in time until the correlation length along the step increases approximately to a value $x$. If $Aq^{\gamma}$ is the dominant regime, we find that Eq. (44) is valid for $t \ll x^{\gamma}/A$. This time depends on the kind of dynamics through $\gamma$ and $A$, and defines the propagation speed of the fluctuations. As expected, the initial fluctuation (44) depends on $x$ and $\tilde{s}$, but not on the kind of dynamics, i.e., $\gamma$ and $A$.

## IV. RESULTS FOR THREE RELAXATION MECHANISMS

First we confirm that our formalism reproduces the known results for the cases of evaporation-condensation and step-edge diffusion, as these cases are quite simple within the context of the formalism we have set up in Secs. II and III. The majority of this section is devoted to mass transport by terrace diffusion, which can produce dynamical correlations between neighboring steps.

Where possible, we compare with prior work, and in doing so, we note that there are three different correlation functions used in the literature. In addition to $G(0,t)$ as defined in Eq. (1), we have

$$w^2(t) = \langle h(0,t)^2 \rangle = G(0,2t),$$

$$\langle (h(0,t) - h(0,0))^2 \rangle = 2G(0,t). \tag{45}$$

$w^2(t)$ describes how the fluctuations of a step grow with time, assuming that the step is initially straight. It is thus a nonequilibrium correlation function. However, within the linear approximation, it is easy to show that $w^2(t) = G(0,2t)$, so that the nonequilibrium and equilibrium correlations are proportional. However, much of the prior analysis has been for the relaxation time $\tau_{pq}$, which does not require the rather tedious inverse Fourier transforms leading to Eq. (24) or the detailed analysis of Sec. III. However, comparison with many of the STM and REM experiments does require the time-dependent correlation functions.

### A. Evaporation-condensation

In this case, there is transport of mass from the surface to the vapor, and from the vapor back to the surface. There is no direct mass transport between adjacent steps. Thus we model this case by a uniform diffusion kernel to the same step and zero diffusion kernel between adjacent steps,

$$P_0(l) = \frac{1}{L}, \quad P_1(l) = 0. \tag{46}$$

Another way to treat evaporation-condensation would be by using $P_0(l) = P_1(l) = 1/(2L)$, which gives the same relaxation time as Eqs. (46). The characteristic time $\tau_h$ is the time between atomic detachment events from a step edge into the vapor. In the simplest case we would expect an activated behavior $\tau_h^{-1} = \tau_{\mathrm{EC}}^{-1} = \nu \exp(-E_{\mathrm{EC}}/k_B T)$, where $\nu$ is a characteristic phonon frequency and $E_{\mathrm{EC}}$ is an evaporation energy. However, this simplified theory remains valid even if many different processes (and barriers) play a role, provided they can be treated as independent. Equation (14) then yields

$$g_0(q) = \frac{\tilde{s} a_\perp}{\tau_{\mathrm{EC}}} q^2, \quad g_1(q) = 0 \tag{47}$$

for all values of $q$. Thus this is the case B [Eq. (28)] of Sec. III without crossover $q_0$, with $A_1 = A_2 = \tilde{s} a_\perp / \tau_{\mathrm{EC}}$ and $\gamma_1 = \gamma_2 = 2$. In the intermediate time regime [Eqs. (40) or (41)], we have

$$G(0,t) = \Omega \left(\frac{a_\perp}{\pi \tilde{s}}\right)^{1/2} \left(\frac{t}{\tau_{\mathrm{EC}}}\right)^{1/2}. \tag{48}$$

This result is essentially the same as that of Bartelt *et al.* [8].

### B. Step-edge diffusion

We restrict diffusion to nearest neighbors along the step edge by defining,

$$P_0(l)=\tfrac{1}{2}\{\delta(l-a_\parallel)+\delta(l+a_\parallel)\},\quad P_1(l)=0. \tag{49}$$

The characteristic time $\tau_h$ is now the time between atomic hopping events between nearest neighbors. We assume a simple activated behavior $\tau_h^{-1}=\nu\exp(-E_{\rm SE}/k_BT)\{\exp(-E_l/k_BT)+\exp(-E_r/k_BT)\}$, where $\nu$ is a characteristic phonon frequency, and $E_{\rm SE}$ the step-edge binding energy, while $E_l$ and $E_r$ are the additional activation barriers that an atom has to overcome to move to the left or right, respectively. In the simplest symmetric case $E_l=E_r=0$; thus $\tau_h^{-1}=2\tau_{\rm SE}^{-1}$ where $\tau_{\rm SE}^{-1}=\nu\exp(-E_{\rm SE}/k_BT)$. Using Eq. (14) then leads to

$$g_0(q)=\frac{2\tilde{s}a_\perp}{\tau_{\rm SE}}q^2\{1-\cos qa_\parallel\},\quad g_1(q)=0. \tag{50}$$

An expansion of $g_0(q)$ at small $q$ yields a behavior like that of case B, with $A_1=\tilde{s}a_\perp a_\parallel^2/\tau_{\rm SE}$, $\gamma_1=4$, and $q_0=1/a_\parallel$. Region $|q|>q_0$ is very small, and has a negligible influence on correlation functions. Thus, in the intermediate time regime we find [using Eq. (41)]

$$G(0,t)=\frac{1}{\pi}\Gamma\left(\frac{3}{4}\right)\left(\frac{\Omega^5 a_\parallel}{\tilde{s}^3}\right)^{\frac{1}{4}}\left(\frac{t}{\tau_{\rm SE}}\right)^{1/4}. \tag{51}$$

This agrees with Bartelt *et al.* [8].

### C. Terrace diffusion

In the terrace diffusion model, an atom detaches onto the terrace below the step edge with probability $p_L$, and onto the terrace above the step edge with probability $p_U$. It then diffuses on the terrace until it reattaches to the same step edge or one of the adjacent step edges. We define $\alpha_L$ to be the sticking coefficient of an atom which approaches a step edge from the lower terrace, and $\alpha_U$ to be the sticking coefficient on approach to the step edge from the upper terrace. We assume simple behavior where $E_{\rm TD}$ is the binding energy, and $E_L$ and $E_U$ are the energy barriers that an atom has to overcome to move to the lower or upper terraces, respectively. $E_L$ and $E_U$ are also energy barriers that an atom has to overcome to stick to the step edge on its approach from the lower and upper terrace, respectively. $E_U$ is the ''Schwoebel barrier.'' In terms of these energies, the detachment probabilites $p_U$ and $p_L$ are the probabilities of detaching

$$p_L=\frac{e^{-E_L/k_BT}}{e^{-E_L/k_BT}+e^{-E_U/k_BT}},\quad p_U=\frac{e^{-E_U/k_BT}}{e^{-E_L/k_BT}+e^{-E_U/k_BT}} \tag{52}$$

and the sticking coefficients (see the Appendix)

$$\alpha_L=\frac{e^{-E_L/k_BT}}{(1-e^{-E_L/k_BT})a_\perp},\quad \alpha_U=\frac{e^{-E_U/k_BT}}{(1-e^{-E_U/k_BT})a_\perp}. \tag{53}$$

The sticking coefficients can have any value in the range $[0,\infty)$, where 0 corresponds to no sticking and $\infty$ to perfect sticking.

Since atoms diffuse on the terrace, $P_0(l)$ and $P_1(l)$ are the probabilities for a random walk on the surface between two fluctuating semisticking walls. The calculation of these probabilities for straight step edges is done in the Appendix:

$$P_0(l)=p_UP(\alpha_U,\alpha_L,d,d-a_\perp,l)+p_LP(\alpha_L,\alpha_U,d,d-a_\perp,l) \tag{54}$$

and

$$P_1(l)=p_UP(\alpha_L,\alpha_U,d,a_\perp,l)+p_LP(\alpha_U,\alpha_L,d,a_\perp,l), \tag{55}$$

where

$$P(\alpha_1,\alpha_2,d,b,l)=\frac{1}{2\pi}\int_{-\infty}^{+\infty}dk\,\frac{\alpha_1(k\cosh kb+\alpha_2\sinh kb)}{(k^2+\alpha_U\alpha_L)\sinh kd+k(\alpha_U+\alpha_L)\cosh kd}\cos kl. \tag{56}$$

These results for two straight edges can be used as the diffusion kernels mediating the dynamics of fluctuation provided the fluctuations are relatively weak (the small slope limit). Integrals (14) may be evaluated to find

$$g_0(q)=\frac{\tilde{s}a_\perp}{\tau_h}q^2\{1-p_Ug(\alpha_U,\alpha_L,d,d-a_\perp,q)-p_Lg(\alpha_L,\alpha_U,d,d-a_\perp,q)\} \tag{57}$$

and

$$g_1(q)=\frac{\tilde{s}a_\perp}{\tau_h}q^2\{p_Lg(\alpha_U,\alpha_L,d,a_\perp,q)+p_Ug(\alpha_L,\alpha_U,d,a_\perp,q)\}, \tag{58}$$

where

$$g(\alpha_1,\alpha_2,d,b,q)=\frac{\alpha_1(q\cosh qb+\alpha_2\sinh qb)}{(q^2+\alpha_U\alpha_L)\sinh qd+q(\alpha_U+\alpha_L)\cosh qd}. \tag{59}$$

Here the characteristic time is related to step edge energies by

$$\tau_h^{-1}=\tau_{\rm TD}^{-1}\{e^{-E_L/k_BT}+e^{-E_U/k_BT}\}, \tag{60}$$

where $\tau_{\rm TD}^{-1}=\nu\exp(-E_{\rm TD}/k_BT)$, and $\nu$ is a characteristic phonon frequency.

In Fig. 2, we plot the spectrum of inverse relaxation times using Eqs. (57) and (58) in Eq. (17) for four different cases: $\alpha_L=\alpha_U=10^3/a_\perp$ (perfect sticking), $\alpha_L=\alpha_U=10^{-2}/a_\perp$ (weak sticking), $\alpha_L=10^3/a_\perp$ and $\alpha_U=10^{-3}/a_\perp$ (finite Schwoebel barrier $E_L\ll E_U$), and $\alpha_L=10^3/a_\perp$ and $\alpha_U=0$ (infinite Schwoebel barrier $E_U\to\infty$). Note in Fig. 2 that, except in the infinite Schwoebel barrier case when there in no atom exchange between the steps, the spectrum of relaxation times is spread between $q^4$ and $q^2$ for small values of $q$. This leads to the step-step correlation in $C_k(x,t)$. On the other hand, the spectrum shrinks to one value (that scales as $q^2$ in weak sticking case, and $q^3$ in perfect sticking and Schwoebel barrier case) for larger values of $q$. In this limit, there is no step-step correlation. Using the spectrum of inverse relaxation times, plotted in Fig. 2, and doing numerical summations over $q$ and $p$, $G(x,t)$ and $C_k(0,t)$, defined by Eqs. (3) and (24), are plotted in Figs. 3 and 4. $G(x,t)$ is plotted for

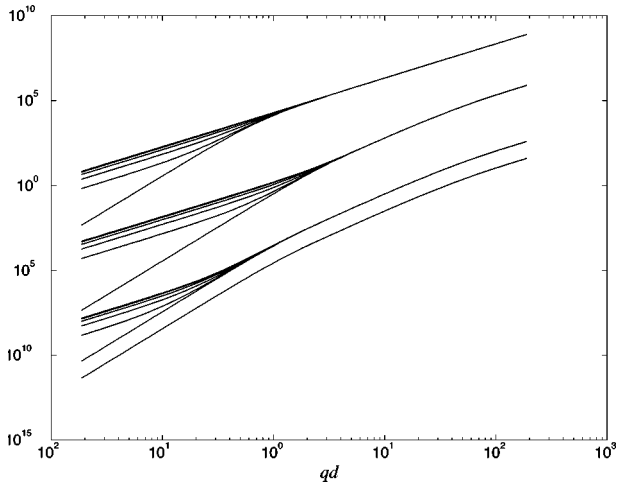


FIG. 2. Inverse relaxation times $1/\tau_{pq}$ in the terrace diffusion case for a surface with $N=10$ steps (due to degeneracy, a maximum of six distinct modes occur); $d=30a_\perp$ and $L=10^4a_\parallel$. We use different ratios $\tilde{s}a_\perp/a_\parallel^2$ for each spectrum to avoid overlapping the spectra. They are plotted for the following sticking coefficients (from the top): $\alpha_L=\alpha_U=10^{-2}/a_\perp$ and $\tilde{s}a_\perp/a_\parallel^2=10^9$; $\alpha_L=\alpha_U=10^3/a_\perp$ and $\tilde{s}a_\perp/a_\parallel^2=10^4$; $\alpha_L^l=10^3/a_\perp$, $\alpha_U^l=10^{-3}/a_\perp$, and $\tilde{s}a_\perp/a_\parallel^2=10$; and $\alpha_L^l=10^3/a_\perp$, $\alpha_U^l=0$, and $\tilde{s}a_\perp/a_\parallel^2=1$. Except in the infinite Schwoebel barrier case (bottom line), the spectrum of relaxation times is spread between $q^4$ and $q^2$ for small values of $q$. On the other hand, the spectrum shrinks to one value (that scales as $q^2$ for the top line, and $q^3$ for the other lines) for larger values of $q$.

the four different cases of the sticking coefficients illustrated in Fig. 2. Each case has a different time scaling. We also show the small time plateau in $G(x,t)$ which exists at finite $x$ [see Eq. (44)]. $C_k(0,t)$ is plotted only for the perfect sticking case for a couple of nonzero values of $k$. Other cases, with nonzero sticking coefficients, show the same scaling. These numerical results are compared to the approximate analytical forms of Tables I–III (see below) which are plotted as dashed lines in Figs. 3 and 4. Those analytical forms, listed in Tables I and II, are obtained by substituting expressions for relaxation times derived below into Eqs. (40), (41), (33), and (35). We also plot $d^2$ as a horizontal dash-dotted line to show when the step fluctuation width exceeds the distance between the steps. Since our model does not include the direct step-step interaction, it fails above the $d^2$ line. Now we derive the limiting forms for the correlation functions $G(0,t)$ and $C_k(0,t)$.

In the limit $q\ll 1/a_\parallel$, expressions (57)–(59) reduce to

$$g_0(q)=\frac{\tilde{s}a_\perp^2}{\tau_{\rm TD}}|q|^3\frac{2\alpha_U\alpha_L\cosh qd+(\alpha_U+\alpha_L)q\sinh qd}{(q^2+\alpha_U\alpha_L)\sinh qd+q(\alpha_U+\alpha_L)\cosh qd} \tag{61}$$

and

$$g_1(q)=\frac{\tilde{s}a_\perp^2}{\tau_{\rm TD}}|q|^3\frac{2\alpha_U\alpha_L}{(q^2+\alpha_U\alpha_L)\sinh qd+q(\alpha_U+\alpha_L)\cosh qd}. \tag{62}$$

These expressions then lead to the relaxation time of a mode of $(p,q)$ according to $\tau_{pq}^{-1}=g_0(q)-g_1(q)\cos p$. Approximate expressions for this relaxation time were found by Pimpinelli *et al.* [9] in a variety of limiting cases, though they implicitly assumed ''in phase motion.'' Khare and Einstein [16] considered in phase and out of phase motion [$A_q\pm 2B_q=g_0(q)\pm g_1(q)$]. In finding the time-dependent correlations, we need the full spectrum (all values of $p$). Ihle, Misbah, and Pierre-Louis [13] also considered the full spectrum, and we reproduce their results for the cases they consider [they only considered $G(0,t)$]. We now discuss limiting cases in which the time dependent correlations may be explicitly evaluated.

*T1 — Terrace diffusion 1* ($d\to\infty$). The large $d$ limit eliminates the flux from neighboring steps, so the steps act independently. In this ''isolated step'' limit, Eqs. (61) and (62) reduce to

$$g_0(q)=\frac{\tilde{s}a_\perp^2}{\tau_{\rm TD}}|q|^3\left(\frac{\alpha_U}{\alpha_U+|q|}+\frac{\alpha_L}{\alpha_L+|q|}\right),\quad g_1(q)=0. \tag{63}$$

Since $g_1(q)=0$, $\tau_{pq}^{-1}=g_0(q)$ and $C_{k\neq 0}(x,t)=0$ (case B). From Eq. (63) it is seen that even isolated steps can have

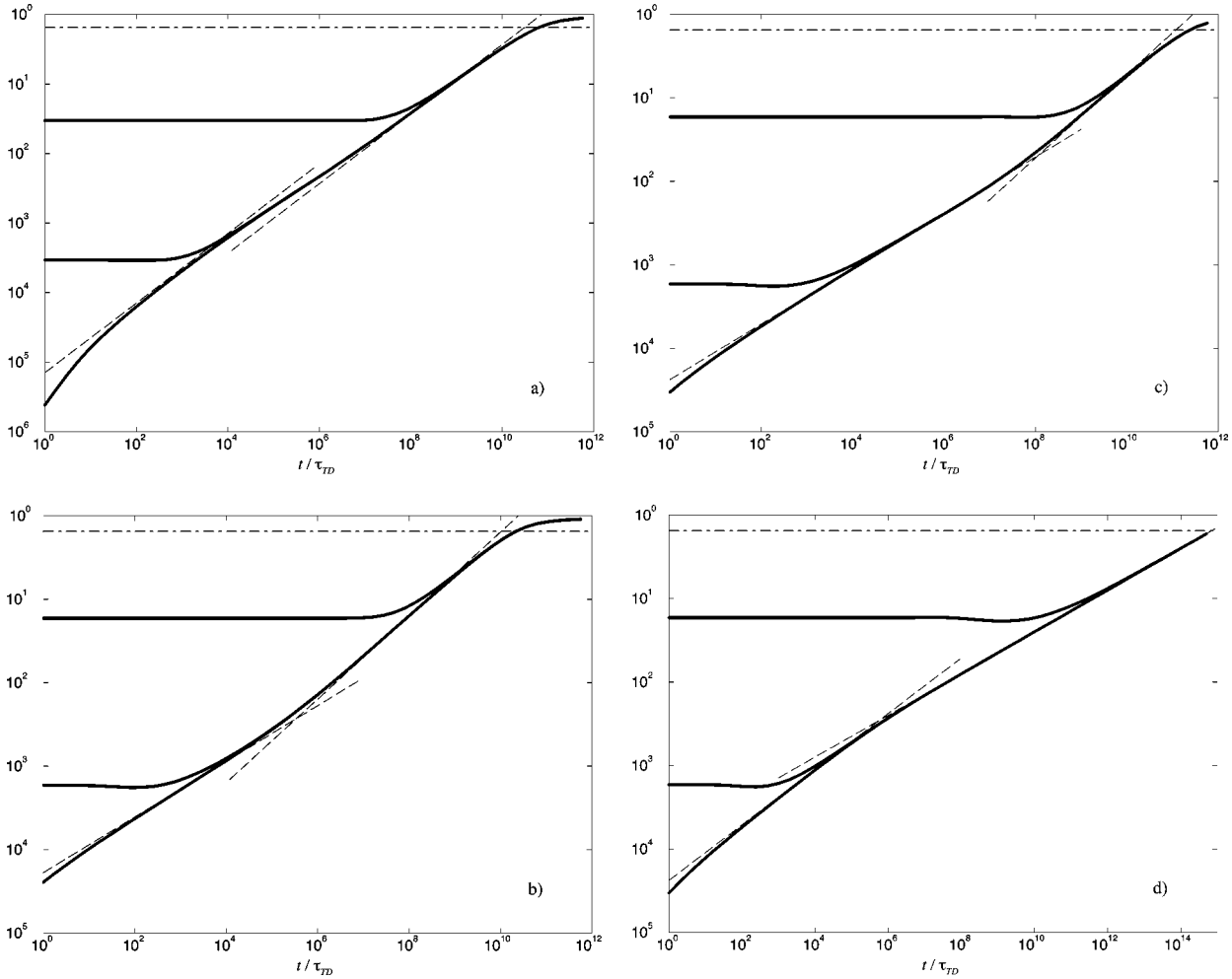


FIG. 3. The autocorrelation function in the case of terrace diffusion. $N=10$, $L=10^5 a_\parallel$, $d=100a_\perp$, and $k_BT/\tilde{\Sigma}=1$. Solid lines are Eq. (3), found from numerical summation of Eq. (24) with Eqs. (57)–(60). Dashed lines are the equations listed in Table I ($0 \ll t \ll \tau_s$), and the horizontal dash-dotted line is $d^2$. The noninteracting approximation we use here is only valid when the correlations are less than $d^2$. The data are for sticking coefficients: (a) $\alpha_L=\alpha_U=10^{-2}/a_\perp$ (case $T3$), and $x=0$, $x=5$, and $x=500$ from the bottom; (b) $\alpha_L=\alpha_U=10^{3}/a_\perp$ (case $T3$), and $x=0$, 10, and 1000 (from the bottom); (c) $\alpha_L=10^{3}/a_\perp$ and $\alpha_U=10^{-3}/a_\perp$ (case $T3$), and $x=0$, 10, and 1000 (from the bottom); (d) $\alpha_L=10^{3}/a_\perp$, and $\alpha_U=0$ (case $T2$), and $x=0$, 10, and 1000 (from the bottom).

three possible regimes: when $|q| \gg \alpha_{U,L}$, then $g_0(q) = \tilde{s}a_\perp^2(\alpha_U+\alpha_L)q^2/\tau_{\rm TD}$ (the $q^2$ dependence for small sticking coefficients was noted in Ref. [10]); when $\alpha_U \ll |q| \ll \alpha_L$ (assuming $\alpha_U \ll \alpha_L$), then $g_0(q)=\tilde{s}a_\perp^2|q|^3/\tau_{\rm TD}$, and when $|q| \ll \alpha_{U,L}$, then $g_0(q)=2\tilde{s}a_\perp^2|q|^3/\tau_{\rm TD}$ (the last expression was derived before [10]). Three different $q$ regimes lead to three different intermediate time regimes in the correlation function $G(0,t)$ as summarized in Table I [using Eqs. (38)–(43)]. After the noninteracting diffuser regime $t \to 0$, there is an early time $0 \ll t \ll t_1^{T1}$ (large $q$ dominant), in which short range processes must overcome the sticking coefficients in order to proceed. For this reason, $\alpha_U+\alpha_L$ appears as a prefactor. This regime is not well defined if $\alpha_{U,L} \to \infty$. In the regime $t_1^{T1} \ll t \ll t_2^{T1}$, one of the terraces (the upper one for the case $\alpha_U \ll \alpha_L$) does not contribute, since the approach to the step edge from that terrace has such a small sticking coefficient. This regime is only well defined if the two sticking coefficients are very different (e.g., the large Schwoebel barrier case, when $\alpha_U \ll \alpha_L$). In the regime $t_2^{T1} \ll t \ll \tau_s^{T1}$, both terraces contribute equally and small sticking coefficients do not play a role. This regime is not well defined if $\alpha_U \approx 0$ or $\alpha_L \approx 0$. Finally, at long enough times, the relaxation is controlled by the slowest mode in the system. Note that these forms apply, at sufficiently short time, even for quite closely spaced steps in a step train, as discussed below.

*T2 — Terrace diffusion 2 (d finite, $\alpha_U=0$ or $\alpha_L=0$).* Setting $\alpha_U=0$ or $\alpha_L=0$ implies that no mass is transported from one step to either of its neighbors (''large barrier limit,'' e.g., the large Schwoebel barrier corresponds to $\alpha_U=0$). At short time (large $q$ dominant), isolated terrace behavior occurs, especially for well separated steps. For small $q$, Eqs. (61) and (62) reduce to

$$g_0(q)=\frac{\tilde{s}da_\perp^2}{\tau_{\rm TD}}q^4, \quad g_1(q)=0; \tag{64}$$

thus $C_{k\neq 0}(x,t)=0$ (case B). The $q^4$ dependence leads to a long time behavior like that of step-edge diffusion, as seen by comparing the correlation functions for this case with that of step edge diffusion (see Table I). The results in Table I are found using Eqs. (41), (43), and (64).

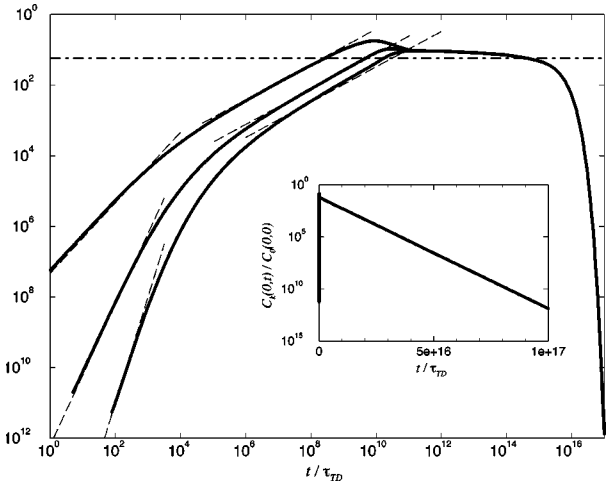


FIG. 4. The step-step correlation function in the terrace diffusion ($T3$) limit. For $N=10$, $L=10^5 a_\parallel$, $d=30a_\perp$, $k_BT/\tilde{\Sigma}=1$, and $\alpha_L=\alpha_U=10^3/a_\perp$. Solid lines are the results of numerical summation of Eq. (24) using Eqs. (57)–(60). Dashed lines are the equations listed in Table II ($t\ll\tau_s$), and the horizontal dash-dotted line is $d^2$. The noninteracting approximation we use here is only valid when the correlations are less than $d^2$. We considered steps separated from each other by $k=1$, 2, and 3 (from the top) intervening steps. The inset is a linear-log plot that shows the exponential time dependence at long times.

*T3 — Terrace diffusion 3* (*d finite*, $\alpha_{U,L}\neq 0$). In this case the $T1$ (isolated step) processes occur at short times (large $q$ dominant). For analysis of the long time behavior (small $q$ dominant), it is useful to define the length

$$d_0=\frac{\alpha_U+\alpha_L}{\alpha_U\alpha_L}. \tag{65}$$

If $d_0$ is finite ($d_0\to\infty$ leads to the $T2$ limit), mass transport between steps is dominant. The approximate forms of Eqs. (61) and (62) for this case are

$$g_0(q)=\frac{\tilde{s}a_\perp^2}{\tau_{\rm TD}}\left(\frac{2}{d+d_0}q^2+dq^4\right),\quad g_1(q)=\frac{2\tilde{s}a_\perp^2}{\tau_{\rm TD}(d+d_0)}q^2, \tag{66}$$

due to the mass transport occurring between steps $g_1(q)\neq 0$, and this is the mathematical origin of a finite value of $C_{k\neq 0}(x,t)$. Results for this limit are summarized in Tables I and II, where we have used $q_0\approx 2/d$ from Fig. 2. This case is probably very important as experimental systems usually satisfy $d\ll L$, so that the diffusion kernels are then affected by adjacent steps. This leads to a correlation between step fluctuations on neighboring steps which becomes the ''signature'' of the $T3$ process. The autocorrelation function $G(0,t)$

TABLE III. Equations for limiting time scales.

| Characteristic time | Physical origin |
|---|---|
| | Evaporation-condensation (EC) |
| $\tau_{\rm EC}=\dfrac{e^{E_{\rm EC}/k_BT}}{\nu}$ | Time related to the binding energy ($E_{\rm EC}$) at the step edge |
| $\tau_s^{\rm EC}=\dfrac{\tau_{\rm EC}}{\tilde{s}a_\perp}\left(\dfrac{L}{2\pi}\right)^2$ | Slowest mode |
| | Step-edge diffusion (SE) |
| $\tau_{\rm SE}=\dfrac{e^{E_{\rm SE}/k_BT}}{\nu}$ | Time related to the binding energy ($E_{\rm SE}$) at the step edge |
| $\tau_s^{\rm SE}=\dfrac{\tau_{\rm SE}}{\tilde{s}a_\perp a_\parallel^2}\left(\dfrac{L}{2\pi}\right)^4$ | Slowest mode |
| | Terrace diffusion (TD) |
| $\tau_{\rm TD}=\dfrac{e^{E_{\rm TD}/k_BT}}{\nu}$ | Time related to the binding energy ($E_{\rm TD}$) at the step edge |
| $\tau_s^{T1}=\dfrac{\tau_{\rm TD}}{2\tilde{s}a_\perp^2}\left(\dfrac{L}{2\pi}\right)^3$ | Slowest mode: terrace diffusion $T1$ (isolated step limit) |
| $\tau_s^{T2}=\dfrac{\tau_{\rm TD}}{d\tilde{s}a_\perp^2}\left(\dfrac{L}{2\pi}\right)^4$ | Slowest mode: terrace diffusion $T2$ (large barrier limit) |
| $\tau_s^{T3}=\dfrac{\tau_{\rm TD}(d+d_0)}{2\tilde{s}a_\perp^2}\left(\dfrac{L}{2\pi}\right)^2$ | Slowest mode: terrace diffusion $T3$ (step to step limit) |
| $t_1^{T1}, t_2^{T1}$ | Crossover times for isolated step limit ($T1$) |
| $t_1^{T2}$ | Crossover time for large barrier limit ($T2$) |
| $t_1^{T3}$ | Crossover time for step to step limit ($T3$) |

(Table I) can have a wide variety of different behaviors. But the pair correlation function only measures the $T3$ process, as it depends on having a finite $g_1(q)$ corresponding to correlated mass transfer between steps. This makes the pair correlation function a useful diagnostic of the dominant surface transport modes.

## V. CONCLUSIONS

We have shown that the pair correlation function between two different steps, $C_{k\neq 0}(x,t)$, can differentiate between terrace diffusion and other surface transport processes, as it is identically zero for the cases of evaporation-condensation and step-edge diffusion. In contrast, $C_{k\neq 0}(x,t)$ is finite and quite large in the case of terrace diffusion. Since $G(0,t)$ is affected by *all mass transport mechanisms*, measurement of $G(0,t)$ and $C_{k\neq 0}(0,t)$ makes it possible to determine the relative importance of terrace diffusion to the other types of mass transport in surface dynamics. The limiting results for $C_{k\neq 0}(0,t)$ and $G(0,t)$ are summarized in Tables I–III, and the general results are in Eqs. (30) and (38). We have also calculated the behavior of $G(x,t)$ for various values of $x$ [see Figs. 3(a)–3(c)]. An experiment in which both $G(x,t)$ and $C_{k\neq 0}(x,t)$ are measured, in combination with a theory like that here, should provide definitive information about the surface mass transport mechanisms.

The analysis here takes a different perspective than that used by previous authors. In particular, we defined a Langevin equation in real space, with ''diffusion kernels'' representing the mass transport processes [see Eq. (6)]. We find this real space picture physically appealing and complementary to the conventional methods [13,16].

## ACKNOWLEDGMENTS

This work was partially supported by the NSF under Grant No. DMR-9312839, and partially by the U.S. DOE under Contract No. DE-FG02-90ER45418.

## APPENDIX: DERIVATION OF $P$ FOR THE TERRACE DIFFUSION CASE

Consider two straight parallel steps 1 and 2 at a distance $d$ from each other. The terrace between the steps is a discrete square lattice defined by $x$ and $y$ axes that are parallel and perpendicular to the steps, repectively. The origin $(x,y)=(0,0)$ is located at distance $a$ from the right of step 1 and at distance $d-a$ from the left of step 2. The energy barriers an atom has to overcome to stick to step 1 or step 2 on approach from the terrace are $E_1$ and $E_2$, respectively. Let us call $p_1(l)$ and $p_2(l)$ the probabilities that an atom will be absorbed at $x=l$ by the step 1 or 2, respectively, after starting a random walk from the origin.

In order to find those probabilities, we can assume that there is a source of atoms, with magnitude $F$, at the origin. After emerging from the source, an atom does a random walk on the terrace until it sticks at a step edge. We define a steady state probability density function for the distribution of the walking atoms on the terrace $\tilde{P}(x,y)$. By knowing $\tilde{P}(x,y)$, $p_1(l)$ and $p_2(l)$ can be found from

$$p_1(l)=a_\perp e^{-E_1/k_BT}\tilde{P}(l,-a+a_\perp),$$

$$p_2(l)=a_\perp e^{-E_2/k_BT}\tilde{P}(l,d-a-a_\perp). \tag{A1}$$

$\tilde{P}(x,y)$ must satisfy the Poisson equation

$$\nabla^2\tilde{P}(x,y)=-F\delta(x)\delta(y). \tag{A2}$$

In addition, it has to satisfy certain boundary conditions at the step edges. These conditions can be derived with the following simple reasoning. Since the probability that an atom, sitting on the site $(x,-a+a_\perp)$, will stick to site $(x,-a)$ on the step edge 1 is $e^{-E_1/k_BT}$, then the probability that it will not stick and bounce back is $1-e^{-E_1/k_BT}$. Thus, effectively, $\tilde{P}(x,-a)\equiv(1-e^{-E_1/k_BT})\tilde{P}(x,-a+a_\perp)$ (see p. 168 of Ref. [22]). Using that and the fact that $\tilde{P}(x,-a+a_\perp)-\tilde{P}(x,-a)\to a_\perp\partial\tilde{P}(x,-a)/\partial y$ for $a_\perp\to 0$, we obtain

$$\frac{\partial\tilde{P}(x,-a)}{\partial y}=\alpha_1\tilde{P}(x,-a), \tag{A3}$$

where notation $\alpha_1\equiv e^{-E_1/k_BT}/(1-e^{-E_1/k_BT})a_\perp$. Similarly, on the other step edge,

$$\frac{\partial\tilde{P}(x,d-a)}{\partial y}=-\alpha_2\tilde{P}(x,d-a), \tag{A4}$$

where $\alpha_2\equiv e^{-E_2/k_BT}/(1-e^{-E_2/k_BT})a_\perp$. $\tilde{P}(x,y)$ can now be found by solving Eq. (A2) with conditions (A3) and (A4).

After calculating $\tilde{P}(x,y)$ (see Appendix C of Ref. [11]), we use Eq. (A1) and normalization

$$2\int_0^{L/2}(p_1(l)+p_2(l))dl=1 \tag{A5}$$

to find $F=a_\perp^{-2}$, and $p_1(l)$ and $p_2(l)$ as

$$p_1(l)=P(\alpha_1,\alpha_2,d,d-a,l),\quad p_2(l)=P(\alpha_2,\alpha_1,d,a,l) \tag{A6}$$

where the function $P$ is written in Eq. (56). Instead of Eq. (A1), we could also use another interesting relationship between $\tilde{P}(x,y)$ and $p_1(l)$ and $p_2(l)$ (after manipulation with above equations):

$$p_1(l)=a_\perp^2\frac{\partial\tilde{P}(x,y=-a)}{\partial y},\ p_2(l)=-a_\perp^2\frac{\partial\tilde{P}(x,y=d-a)}{\partial y}. \tag{A7}$$

[1] A recent set of minireviews is contained in *Dynamics of Crystal Surfaces and Interfaces*, edited by P.M. Duxbury and T.J. Pence (Plenum, New York, 1997).

[2] X.S. Wang, J.L. Goldberg, N.C. Bartelt, T.L. Einstein, and E.D. Williams, Phys. Rev. Lett. **65**, 2430 (1990).

[3] B. Swartzentruber, Y.W. Mo, R. Kariotis, M.G. Lagally, and M.B. Webb, Phys. Rev. Lett. **65**, 1913 (1990).

[4] M. Poensgen, J.F. Wolf, J. Frohn, M. Giesen, and H. Ibach, Surf. Sci. **274**, 430 (1992).

[5] N.C. Bartelt, J.L. Goldberg, T.L. Einstein, E.D. Williams, J.C. Heyraud, and J.J. Métois, Phys. Rev. B **48**, 15 453 (1993)

[6] L. Kuipers, M.S. Hoogeman, and J.W.M. Frenken, Phys. Rev. Lett. **71**, 3517 (1993).

[7] M. Giesen-Seibert, F. Schmitz, R. Jentjens, and H. Ibach, Surf. Sci. **329**, 47 (1995).

[8] N.C. Bartelt, J.L. Goldberg, T.L. Einstein, and E.D. Williams, Surf. Sci. **273**, 252 (1992). To compare the results, make the substitutions $\tilde{\Sigma}\rightarrow\tilde{\gamma}$, $\tau_{\mathrm{EC(SE)}}\rightarrow\tau_{a(h)}$, and $G(0,2t)\rightarrow w^2(t)$.

[9] A. Pimpinelli, J. Villain, D.E. Wolf, J.J. Métois, J.C. Heyraud, I. Elkinani, and G. Uimin, Surf. Sci. **295**, 143 (1993).

[10] N.C. Bartelt, T.L. Einstein, and E.D. Williams, Surf. Sci. **312**, 411 (1994). To compare the results, make the substitutions $\tilde{\Sigma}\rightarrow\tilde{\beta}$ and $a_\perp^2/\tau_{\mathrm{TD}}\rightarrow D_s c_0\Omega$.

[11] B. Blagojević and P.M. Duxbury, in *Dynamics of Crystal Surfaces and Interfaces* [1].

[12] S.V. Khare and T.L. Einstein, in *Dynamics of Crystal Surfaces and Interfaces* [1].

[13] T. Ihle, C. Misbah, and O. Pierre-Louis, Phys. Rev. B **58**, 2289 (1998). To compare the results make the substitutions $\tilde{\Sigma}\rightarrow\gamma$, $\alpha_U\rightarrow d_+^{-1}$, $\alpha_L\rightarrow d_-^{-1}$, and $a_\perp^2/\tau_{\mathrm{TD}}\rightarrow Dc_{\mathrm{eq}}^0\Omega$. Also, in their expressions, set $A=0$, $B=0$, and $x_s\rightarrow\infty$, since the theory presented here does not include step interactions, and step-edge diffusion and evaporation acting together with terrace diffusion.

[14] H.P. Bonzel and W.W. Mullins, Surf. Sci. **350**, 285 (1996); H.P. Bonzel and S. Surnev, in *Dynamics of Crystal Surfaces and Interfaces* [1]. Several other articles in Ref. [1] also treated this topic.

[15] W. Selke and P.M. Duxbury, Phys. Rev. B **52**, 17 468 (1995).

[16] S.V. Khare and T.L. Einstein, Phys. Rev. B **57**, 4782 (1998). To compare the results, make the substitutions $\tilde{s}\rightarrow S$, $\tilde{\Sigma}\rightarrow\tilde{\beta}$, $\alpha_U\rightarrow k_-/D_{\mathrm{su}}$, $\alpha_L\rightarrow k_+/D_{\mathrm{su}}$, and $a_\perp^2/\tau_{\mathrm{TD}}\rightarrow D_{\mathrm{su}}$. Also, in their expressions, set $D_{\mathrm{st}}=0$, since the theory presented here does not include coupling of step-edge diffusion to terrace diffusion.

[17] W.W. Mullins, in *Metal Surfaces: Structure, Energetics and Kinetics*, edited by R. Vanselow and R. Howe (Springer, New York, 1963).

[18] P.J. Davis, *Circulant Matrices* (Wiley, New York, 1979).

[19] P. Nozières, in *Solids Far from Equilibrium*, edited by C. Godrèche (Cambridge University Press, Cambridge, 1991).

[20] M. Abramowitz and I.A. Stegun, *Handbook of Mathematical Functions*, (Dover, New York, 1972).

[21] I.S. Gradshteyn and I.M. Ryzhik, *Table of Integrals, Series, and Products* (Academic Press, New York, 1965).

[22] G.H. Weiss, *Aspects and Applications of the Random Walk* (North-Holland, Amsterdam, 1994).